NATIONAL ADVISORY COMMITTEE
FOR AERONAUTICS

REPORT No. 475

WING PRESSURE DISTRIBUTION
AND ROTOR-BLADE MOTION OF AN AUTOGIRO
AS DETERMINED IN FLIGHT

By JOHN B. WHEATLEY

1933

AERONAUTICAL SYMBOLS

1. FUNDAMENTAL AND DERIVED UNITS

	Symbol	Metric		English	
		Unit	Symbol	Unit	Symbol
Length	l	meter	m	foot (or mile)	ft. (or mi.)
Time	t	second	s	second (or hour)	sec. (or hr.)
Force	F	weight of 1 kilogram	kg	weight of 1 pound	lb.
Power	P	kg/m/s		horsepower	hp.
Speed		$\begin{cases} \text{km/h} \\ \text{m/s} \end{cases}$	k.p.h. m.p.s.	mi./hr ft./sec	m.p.h. f.p.s.

2. GENERAL SYMBOLS, ETC.

W, Weight $= mg$

g, Standard acceleration of gravity $= 9.80665$ m/s^2 $= 32.1740$ ft./sec.^{2}

m, Mass $= \dfrac{W}{g}$

ρ, Density (mass per unit volume).

Standard density of dry air, 0.12497 (kg-m^{-4} s^2) at 15° C. and 750 mm $= 0.002378$ (lb.-ft.$^{-4}$ sec.^{2}).

Specific weight of "standard" air, 1.2255 kg/m^3 $= 0.07651$ lb./ft.^{3}.

mk^2, Moment of inertia (indicate axis of the radius of gyration k, by proper subscript).

S, Area.

S_w, Wing area, etc.

G, Gap.

b, Span.

c, Chord.

$\dfrac{b^2}{S}$, Aspect ratio.

μ, Coefficient of viscosity.

3. AERODYNAMICAL SYMBOLS

V, True air speed

q, Dynamic (or impact) pressure $= \dfrac{1}{2}\rho V^2$.

L, Lift, absolute coefficient $C_L = \dfrac{L}{qS}$

D, Drag, absolute coefficient $C_D = \dfrac{D}{qS}$

D_o, Profile drag, absolute coefficient $C_{Do} = \dfrac{D_o}{qS}$

D_i, Induced drag, absolute coefficient $C_{Di} = \dfrac{D_i}{qS}$

D_p, Parasite drag, absolute coefficient $C_{Dp} = \dfrac{D_p}{qS}$

C, Cross-wind force, absolute coefficient $C_C = \dfrac{C}{qS}$

R, Resultant force.

i_w, Angle of setting of wings (relative to thrust line).

i_t, Angle of stabilizer setting (relative to thrust line).

Q, Resultant moment.

Ω, Resultant angular velocity.

$\rho\dfrac{Vl}{\mu}$, Reynolds Number, where l is a linear dimension.

e.g., for a model airfoil 3 in. chord, 100 mi./hr. normal pressure, at 15° C., the corresponding number is 234,000; or for a model of 10 cm chord 40 m/s, the corresponding number is 274,000.

C_p, Center of pressure coefficient (ratio of distance of c. p. from leading edge to chord length).

α, Angle of attack.

ϵ, Angle of downwash.

α_o, Angle of attack, infinite aspect ratio

α_i, Angle of attack, induced.

α_a, Angle of attack, absolute. (Measured from zero lift position.)

γ, Flight path angle.

REPORT No. 475

WING PRESSURE DISTRIBUTION
AND ROTOR-BLADE MOTION OF AN AUTOGIRO
AS DETERMINED IN FLIGHT

By JOHN B. WHEATLEY

Langley Memorial Aeronautical Laboratory

NATIONAL ADVISORY COMMITTEE FOR AERONAUTICS

NAVY BUILDING, WASHINGTON, D.C.

(An independent Government establishment, created by act of Congress approved March 3, 1915, for the supervision and direction of the scientific study of the problems of flight. Its membership was increased to 15 by act approved March 2, 1929 (Public, No. 908, 70th Congress). It consists of members who are appointed by the President, all of whom serve as such without compensation.)

JOSEPH S. AMES, Ph.D., *Chairman*,
    President, Johns Hopkins University, Baltimore, Md.
DAVID W. TAYLOR, D.Eng., *Vice Chairman*,
    Washington, D.C.
CHARLES G. ABBOT, Sc.D.,
    Secretary, Smithsonian Institution, Washington, D.C.
LYMAN J. BRIGGS, Ph.D.,
    Director, Bureau of Standards, Washington, D.C.
ARTHUR B. COOK, Captain, United States Navy,
    Assistant Chief, Bureau of Aeronautics, Navy Department, Washington, D.C.
WILLIAM F. DURAND, Ph.D.,
    Professor Emeritus of Mechanical Engineering, Stanford University, California.
BENJAMIN D. FOULOIS, Major General, United States Army,
    Chief of Air Corps, War Department, Washington, D.C.
HARRY F. GUGGENHEIM, M.A.,
    Port Washington, Long Island, New York.
ERNEST J. KING, Rear Admiral, United States Navy,
    Chief, Bureau of Aeronautics, Navy Department, Washington, D.C
CHARLES A. LINDBERGH, LL.D.,
    New York City.
WILLIAM P. MACCRACKEN, Jr., Ph.B.,
    Washington, D.C.
CHARLES F. MARVIN, Sc.D.,
    Chief, United States Weather Bureau, Washington, D.C.
HENRY C. PRATT, Brigadier General, United States Army,
    Chief, Matériel Division, Air Coprs, Wright Field, Dayton, Ohio.
EDWARD P. WARNER, M.S.,
    Editor "Aviation," New York City.
ORVILLE WRIGHT, Sc.D.,
    Dayton, Ohio.

GEORGE W. LEWIS, *Director of Aeronautical Research.*
JOHN F. VICTORY, *Secretary.*
HENRY J. E. REID, *Engineer in Charge, Langley Memorial Aeronautical Laboratory, Langley Field, Va.*
JOHN J. IDE, *Technical Assistant in Europe, Paris, France.*

EXECUTIVE COMMITTEE

JOSEPH S. AMES, *Chairman.*
DAVID W. TAYLOR, *Vice Chairman.*

CHARLES G. ABBOT.   WILLIAM P. MACCRACKEN, Jr.
LYMAN J. BRIGGS.   CHARLES F. MARVIN.
ARTHUR B. COOK.   HENRY C. PRATT.
BENJAMIN D. FOULOIS.   EDWARD P. WARNER.
ERNEST J. KING.   ORVILLE WRIGHT.
CHARLES A. LINDBERGH.

JOHN F. VICTORY, *Secretary.*

Report No. 475

WING PRESSURE DISTRIBUTION AND ROTOR-BLADE MOTION OF AN AUTOGIRO AS DETERMINED IN FLIGHT

By John B. Wheatley

SUMMARY

This report presents the results of tests in which the pressure distribution over the fixed wing of an autogiro was determined in both steady and accelerated flight. In the steady-flight condition, the rotor-blade motion was also measured. These data show that in steady flight the rotor speed as a function of the air speed is largely affected by the variation of the division of load between the rotor and the wing; as the load on the wing increases, the rotor speed decreases. In steady flight the presence of the slipstream increased both the wing lift at a given air speed and the maximum lift coefficient of the wing above the corresponding values without the slipstream. In abrupt high-speed turns, the wing attained a normal-force coefficient of unity at almost the initial value of the air speed and experienced its maximum load before maximum acceleration occurred.

INTRODUCTION

The distinctive characteristic of the autogiro is that lift is developed by a rotor consisting of a windmill of low pitch having a number of blades articulated at the axis of rotation to permit an oscillation without mechanical constraint in planes containing the axis of rotation. In the complete machine, this type of lifting device is usually combined with a fixed wing of normal type which produces a considerable portion of the total lift. A determination of the loads on the normal, or fixed, wing of the autogiro has become desirable because of the need for establishing rational design rules for the wing itself, and also because it is necessary to know the division of load between rotor and wing in order to study the aerodynamic characteristics of the rotor. This study of the rotor requires, in addition, that the motion of the blades about their points of articulation be determined and correlated with the lift developed by the rotor.

There are presented herein the results of flight tests in which the division of load between the rotor and fixed wing of an autogiro was determined during steady and accelerated conditions; in steady flight, the rotor-blade motion was also obtained. The wing normal force was determined by means of pressure-distribution measurements, the rotor lift being calculated as the difference between the total lift and the calculated wing lift. The blade motion was measured by means of a motion-picture camera on the rotor hub, which photographed one blade during rotation. The tests were made with a Pitcairn PCA-2 autogiro at Langley Field, Va., during 1932 and 1933. The aerodynamic characteristics of this autogiro had been previously determined and reported in reference 1.

A further development in connection with this investigation is the application of the data concerning the rotor to an analysis of the aerodynamic theory of the autogiro rotor as presented by Lock (reference 2). The results of this study are soon to be published.

GENERAL CONSIDERATIONS

The aerodynamic analysis of the autogiro rotor is given in detail in reference 2, but certain fundamental considerations will be briefly discussed here. In this and related types of rotating-wing systems, the lift and drag coefficients based on speed of translation, the blade motion, and the angle of attack are uniquely determined by the tip-speed ratio μ. The tip-speed ratio is the quotient of the component of the speed of translation in the plane of the rotor disk and the tip-speed of the rotor, and is expressed by the equation

$$\mu = \frac{V \cos \alpha}{\Omega R}$$

where V is the true air speed
  α is the rotor angle of attack
  Ω is the rotor angular velocity
  R is the rotor radius

The explanation of the dependence of the blade motion upon μ is relatively simple. The rotor blades, being free to oscillate as they rotate, follow a path that tends to balance the moment of the thrust against the

3

moment of the centrifugal force. The blade rotating into the wind will sustain an increase in thrust and will rise, which increases the centrifugal moment and decreases the thrust; the opposing blade meanwhile has sustained a decrease in thrust and falls, which decreases the centrifugal moment and increases the thrust. The motion is directly due to the difference in velocities on opposite portions of the rotor disk, and is consequently a function of μ. It is impossible to explain briefly the dependence of the force coefficients upon μ, since the relations are not obvious and are extremely complicated. The expressions for the force coefficients are given in reference 2.

The instantaneous position of a blade is completely defined when the azimuth angle ψ of the blade-span axis, projected onto the rotor disk, is given and the
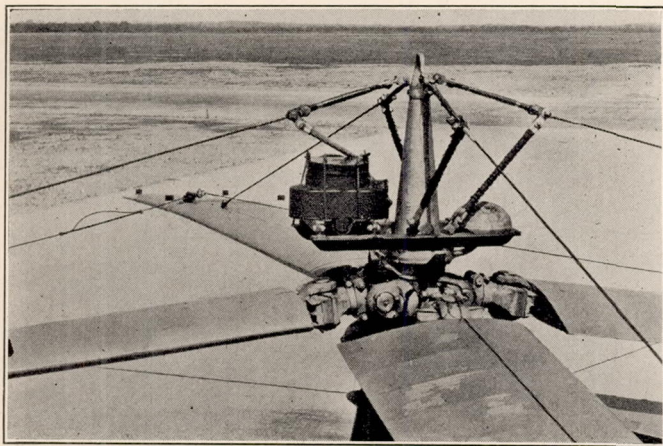

FIGURE 1.—PCA-2 autogiro.

FIGURE 2.—Installation of motion-picture camera on hub of PCA-2 autogiro.

angle β between the blade-span axis and the plane of the disk is known. Since at a given value of μ the blade follows the same path every revolution, the angle β is conveniently expressed as a Fourier series in ψ, which is measured from the downwind position. The equation is

$$\beta = a_0 - a_1 \cos \psi - b_1 \sin \psi - a_2 \cos 2 \psi - b_2 \sin 2 \psi - a_3 \cos 3 \psi - b_3 \sin 3 \psi - \ldots \ldots$$

where β is the angle between the blade span axis and the plane of the rotor disk

and a_n and b_n are the Fourier constants representing the blade motion, and are functions of μ.

The results of tests of the blade motion are presented in this report as the coefficients a_0, a_1, b_1, a_2, and b_2 as

functions of μ, which completely define the instantaneous position of a blade for a given tip-speed ratio. Coefficients of higher order than a_2 and b_2 were found to be negligible, being less than the probable experimental error.

APPARATUS AND METHODS

The autogiro used in these tests was a Pitcairn PCA-2 (fig. 1) having the following dimensions and characteristics:

Gross weight	2,980 lbs.
Number of blades on rotor	4.
Profile of rotor blade section	Göttigen 429.
Rotor radius	22.5 ft.
Area of 1 blade	38.6 sq. ft.
Blade weight	79 lbs.
Blade center of gravity—distance from horizontal hinge	9.73 ft.
Moment of inertia of blade about horizontal hinge	334 slug ft.[2]
Wing profile	Modified M-3.
Wing span	30.3 ft.
Wing area projected (N.A.C.A. convention)	101 sq. ft.
Incidence of wing to rotor disk	3.6°.

The required measurements for the steady-flight conditions were obtained from synchronized records of the dynamic pressure, the attitude angle, the rate of change of static pressure, the pressures on the fixed wings, the rotor speed, and the rotor blade angles. Standard N.A.C.A. photographic-recording instruments were used for most of these measurements. The dynamic pressure was recorded with an air-speed recorder, the attitude angle with a pendulum-type inclinometer, and the wing pressures by means of two multiple manometers. The change in static pressure was measured with a recording statoscope, which consisted of an air-speed pressure cell having one side of the diaphragm connected to a closed chamber and the other side open to cockpit pressure. Rotor speed was determined by a recording instrument in which the source light was connected to an electrical circuit that was closed once each revolution of the rotor. A timer was utilized to provide time scales on the records obtained with the above-mentioned instruments.

The problem of measuring the rotor-blade motion was solved by fixing a motion-picture camera to the rotor hub so that one rotor blade was in the field of the camera. Small targets were attached to the leading and trailing edges of a blade at 50 and 75 percent of the radius, and the position of these targets in the camera field was used to determine the angle of the span axis of the blade to the rotor disk. The photographs were oriented in azimuth by including the tail surfaces of the autogiro in the camera field. By this method, the azimuth angle of one frame per revolution was fixed, and the remaining frames were oriented by assuming the camera speed constant. A photograph of the camera installation and targets is shown in figure 2.

The quantities necessary to determine the tip-speed ratio are dynamic pressure, air density, angle of attack, and rotor speed. The air density was found by visual observations of an indicating altimeter in the autogiro and observations of ground temperature, assuming a gradient of $-3°$ F. per thousand feet. The angle of attack was determined as the difference between the attitude and the flight-path angles, the flight-path angle being calculated from the true air speed and the rate of change of static pressure with time.

In accelerated flight, measurements were made of wing-pressure distribution, dynamic pressure, and normal acceleration. An N.A.C.A. 3-component accelerometer was used to determine the three components of the resultant acceleration. An attempt was made to measure the rotor-blade motion in accelerated flight, but the rotor speed changed so rapidly that the orientation of the photographs proved impossible. Furthermore, even with a lens having an angle of 50°, the necessity for including the tail surfaces in the camera field resulted in the blades passing outside the field when the normal acceleration became large.

were made simultaneously over both wing panels, using both manometers, to determine accurately any accidental asymmetry of loading.

The flight tests consisted of a series of steady glides with engine fully throttled at speeds over the entire flight range; a series of level flight runs and full-throttle climbs at several air speeds; and a number of steady full-throttle turns at air speeds in the vicinity of the speed for minimum radius of turn. Accelerated-flight tests consisted of several abrupt turns at air speeds varying from 106 to 136 miles per hour; for reasons given in the discussion, no maneuvers in a vertical plane were made. Except in the abrupt turns, all measured quantities were obtained as the average of a 10-second run. In the abrupt turns, the continuous records of the measured quantities were read at every quarter second and smooth curves then drawn through the resultant points.

RESULTS

The results of the tests are presented in figures 4 to 22 and in tables I, II, and III. Figures 4 to 14 and
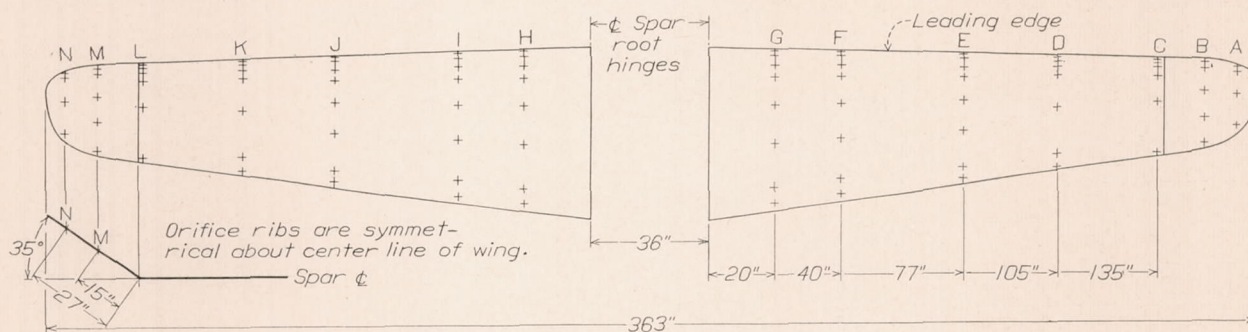
ORIFICE POSITIONS

[In inches from leading edge]

Orifice no.	Rib A. N	Rib B. M	Rib C. L	Rib D. K	Rib E. J	Rib F. I	Rib G. H
1	1	$1\frac{3}{32}$	$\frac{3}{4}$	$\frac{3}{4}$	$\frac{3}{4}$	$\frac{3}{4}$	$1\frac{5}{16}$
2	$2\frac{3}{32}$	$2\frac{11}{16}$	$1\frac{7}{32}$	$1\frac{13}{32}$	$1\frac{5}{8}$	$1\frac{13}{16}$	$1\frac{15}{16}$
3	$9\frac{7}{16}$	$9\frac{7}{16}$	$3\frac{1}{32}$	$3\frac{1}{2}$	$4\frac{3}{32}$	$4\frac{9}{16}$	$4\frac{7}{8}$
4	$18\frac{15}{16}$	$17\frac{9}{16}$	$5\frac{15}{32}$	$6\frac{5}{16}$	$7\frac{3}{8}$	$8\frac{7}{32}$	$8\frac{25}{32}$
5		$25\frac{5}{8}$	$13\frac{5}{8}$	$15\frac{13}{16}$	$14\frac{5}{16}$	$15\frac{13}{16}$	$17\frac{1}{8}$
6			$28\frac{3}{4}$	$29\frac{13}{16}$	$23\frac{1}{2}$	$26\frac{1}{2}$	$28\frac{1}{2}$
7				$33\frac{11}{32}$	$34\frac{3}{4}$	$38\frac{3}{4}$	$41\frac{1}{2}$
8					$38\frac{3}{4}$	$43\frac{5}{16}$	$46\frac{3}{8}$
Chord of rib, inches	21	27	$30\frac{5}{16}$	$35\frac{1}{8}$	$40\frac{3}{4}$	$45\frac{9}{16}$	$48\frac{13}{16}$

FIGURE 3.—Layout of orifices in PCA-2 autogiro wing.

The layout of orifices used in the measurements of wing pressures is shown in figure 3, the orifices being connected to the manometer so that the differences between the pressures on the top and bottom surfaces were recorded. During the steady-flight tests, pressures were measured over the whole of the left-wing panel and on ribs C and G of the right panel, one 60-cell manometer being used. After the addition of a 30-cell manometer, tests were made to obtain the total wing load as a function of the left-panel load. In accelerated flight, the measurements of wing pressures

tables I and II summarize the results obtained in steady flight, and figures 15 to 22 present time histories of measured quantities in abrupt turns and curves showing the maximum span load encountered in each turn. In table III, orifice pressures have been tabulated for the maximum speed obtained in a steady glide and for the maximum wing load obtained in the abrupt turns.

The force coefficients used in the results are differentiated by appropriate subscripts; thus, C_{L_r} is the lift coefficient of the rotor, C_{N_r} is the normal-force coeffi-

cient of the rotor, C_{L_w} is the lift coefficient of the wing, etc. The values of the wing lift and normal-force coefficients were obtained by fairing the span-load curve smoothly between the points adjacent to the fuselage, to determine the total wing load, and using
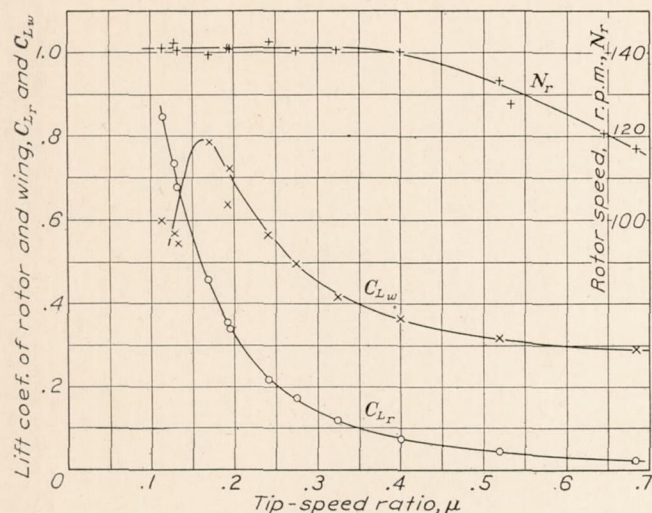
rotor force coefficients are based on the swept disk area πR^2. (See reference 1.)

FIGURE 4.—Rotor speed and lift coefficients of rotor and wing—gliding flight (PCA-2 autogiro).

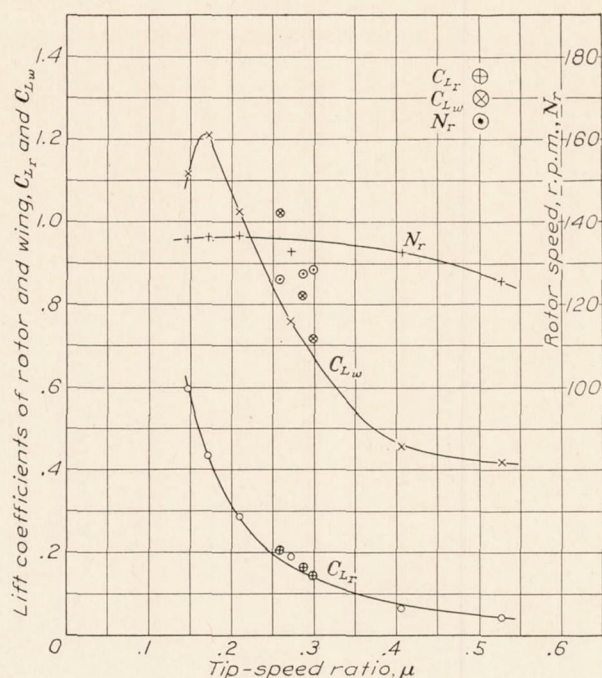FIGURE 7.—Rotor speed and lift coefficients of rotor and wing—level flight and climb (PCA-2 autogiro).

NOTE.—Faired curves show level-flight results. Points obtained in climbs shown by symbols.

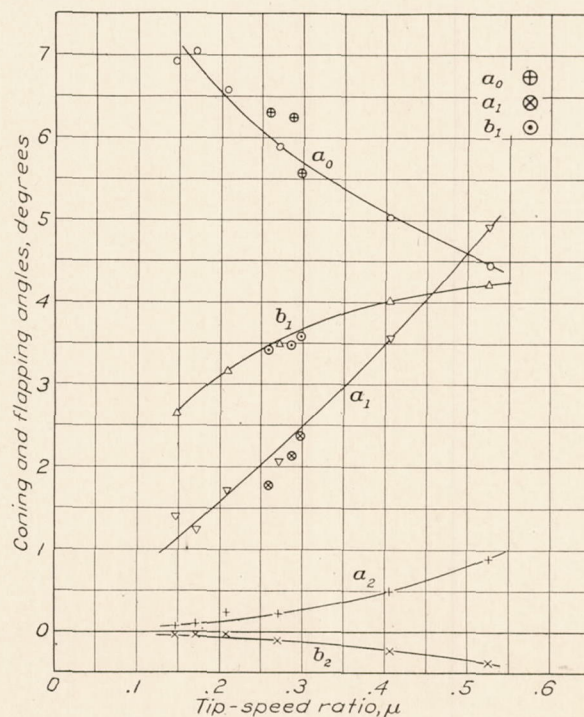FIGURE 5.—Coning and flapping angles—gliding flight (PCA-2 autogiro).

FIGURE 8.—Coning and flapping angles—level flight and climb (PCA-2 autogiro).

NOTE.—Faired curves show level-flight results. Points obtained in climbs shown by symbols.

a wing area obtained by assuming that the wing extends through the fuselage with a chord equal to its root chord. This practice is conventional, having been adopted by the N.A.C.A. to take into account approximately the load carried by the fuselage. The

It will be noted that for the accelerated-flight condition, the coefficients used were based on normal

force, while for steady flight the lift force was used. As design criterions are usually given in terms of normal force, the accelerated-flight results may be directly applied to this purpose. The results from the steady-flight tests, however, are to be used for purposes of aerodynamic analysis, in which case the lift is more useful than the normal force. The lift force was calculated from measured values of the normal force, angle of attack, and flight-path angle by a simple resolution, and chord forces on the wing were considered to be negligible components of the lift.

PRECISION

Steady flight.—Accidental errors arising from changes in instrument calibrations were almost entirely eliminated by frequent calibrations. Additional errors caused by variations in the values of the measured quantities during a run were minimized by using the average over the full 10-second duration of the run; in general, however, the runs were so steady that this
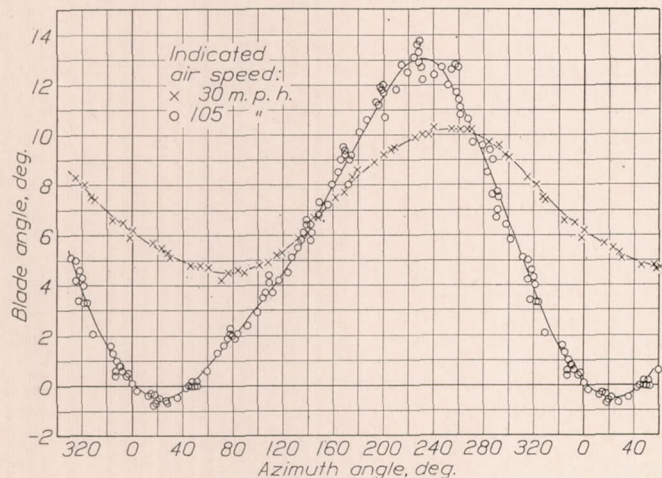

FIGURE 6.—Typical data for blade-angle measurements (PCA-2 autogiro).

type of error could be entirely neglected. The position error of the air-speed head was determined in a speed-course calibration in level flight; the lag characteristics of the static and pressure tubing were then equalized so that no error would arise from varying static pressure.

The motion-picture-camera records were read to the closest 0.1° blade angle, the camera being oriented in azimuth to within ±1.0°. The curve of blade angle against azimuth angle was defined in every case by at least 100 points, to reduce accidental errors to a small quantity. The consistent results obtained by the test procedure are demonstrated by the typical curves shown in figure 6.

The precision of the final results in the form of faired curves is summarized as follows:

$$\mu \quad \pm 3 \text{ percent}$$
$$C_{L_r} \quad \pm 3 \text{ percent}$$
$$C_{L_w} \quad \pm 3 \text{ percent}$$
$$\text{Fourier coefficients} \quad \pm 0.1°$$

Accelerated flight.—The air-speed calibration obtained in steady flight does not apply rigorously to the
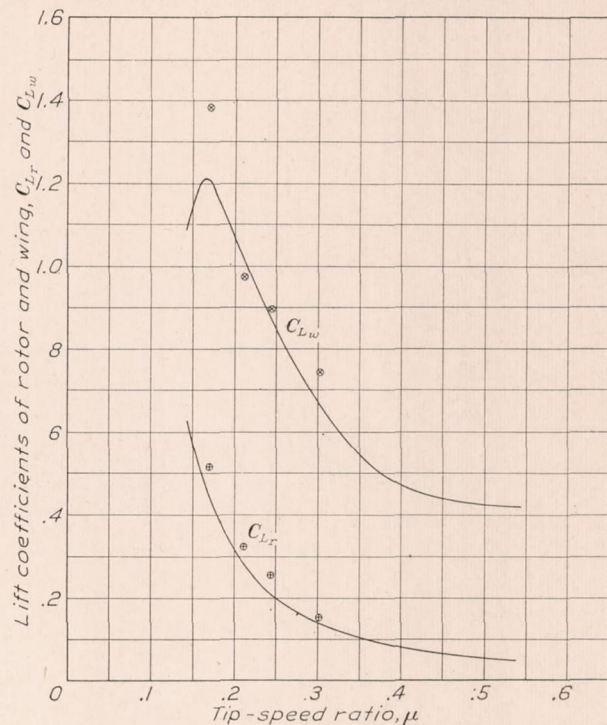

FIGURE 9.—Lift coefficients of rotor and wing—level flight, steady turns (PCA-2 autogiro).

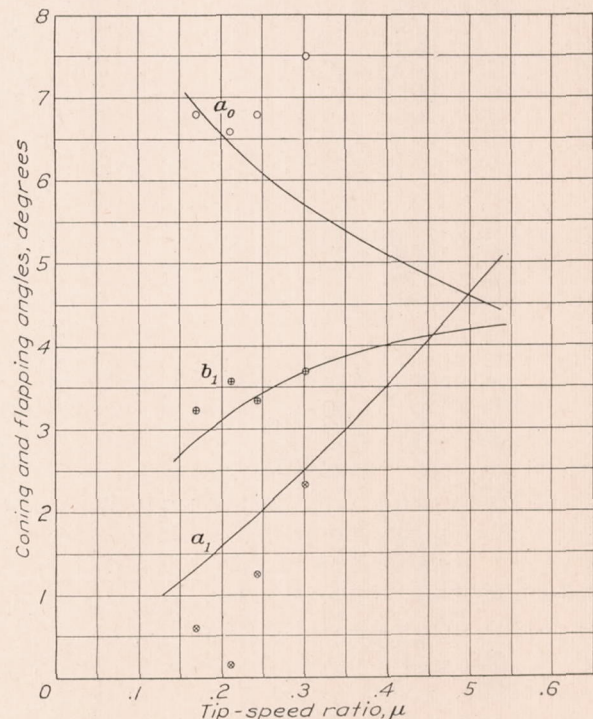NOTE.—Faired curves are level-flight results. Points are for turns.

FIGURE 10.—Coning and flapping angles—level flight, steady turns (PCA-2 autogiro).

NOTE.—Faired curves are level-flight results. Points are for turns.

accelerated-flight condition because air speed is not then a unique function of angle of attack. It is impossible to evaluate quantitatively the error so introduced,

but it is not considered serious, since the corrections required in steady flight to change recorded to correct dynamic pressure were small. The over-all precision of the accelerated-flight results is expressed by the following:

$$\text{Normal acceleration } \pm 0.05 \text{ g}$$
$$C_{N_r} \pm 4 \text{ percent}$$
$$C_{N_w} \pm 4 \text{ percent}$$

DISCUSSION

Steady flight.—The effect of the slipstream on the wing characteristics is illustrated by the difference be-
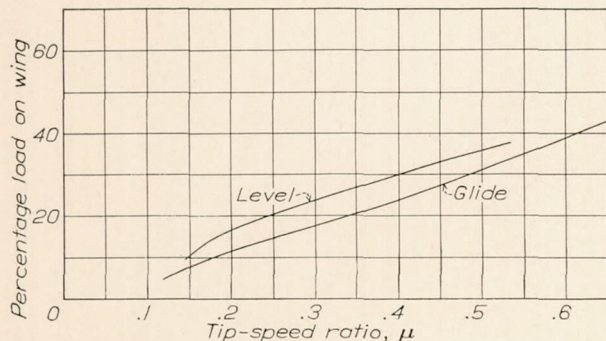

FIGURE 11.—Variation of rotor-wing load division with tip-speed ratio—level flight and glide (PCA-2 autogiro).
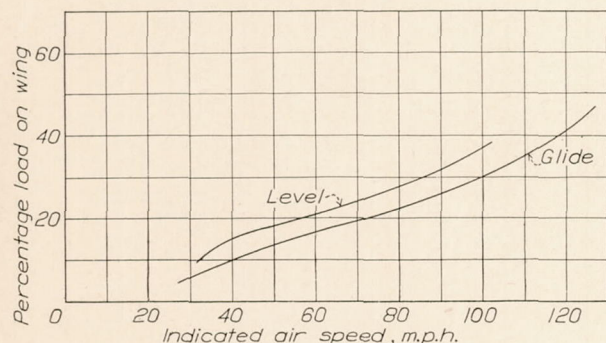

FIGURE 12.—Variation of rotor-wing load division with air speed—level flight and glide (PCA-2 autogiro.)

tween the values of the wing lift coefficient in a glide and in level flight at equal values of the tip-speed ratio. (See figs. 4 and 7.) The rotor lift coefficient shown in the same figures is unaffected within the limits of experimental error. It is particularly interesting to note the marked difference between the maximum lift coefficients of the wing in the two conditions, a difference which is probably due partly to the increased dynamic pressure in the slipstream and partly to such indeterminate factors as turbulence and change in angle of flow behind the propeller. The augmented wing load in the wake of the propeller is shown in figures 13 and 14. The peak of the lift curve in figures 4 and 7 apparently occurs at the same tip-

speed ratio, consequently the same angle of attack, in both cases.

The load division between rotor and wing is shown in figure 11 as a function of tip-speed ratio and in figure 12 as a function of air speed. In reference 2, it is shown that rotor speed at a given tip-speed ratio is proportional to the square root of the load carried by the rotor, so the decrease in rotor speed at large tip-speed ratios, which is shown in figures 4 and 7, can be ascribed at least in part to the corresponding decrease in rotor load.

A complete discussion of the significance of the data concerning the blade motion is not attempted at this
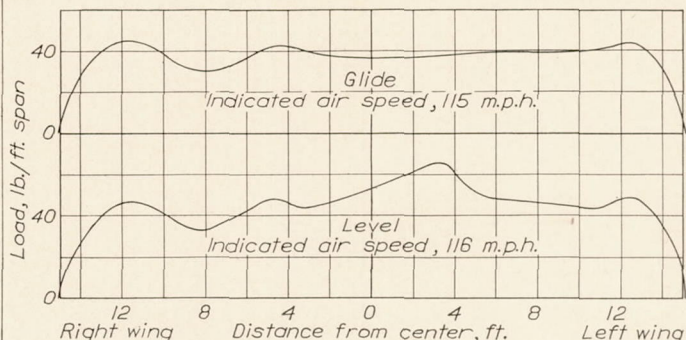
FIGURE 13.—Typical span-load curves—high speed (PCA-2 autogiro).
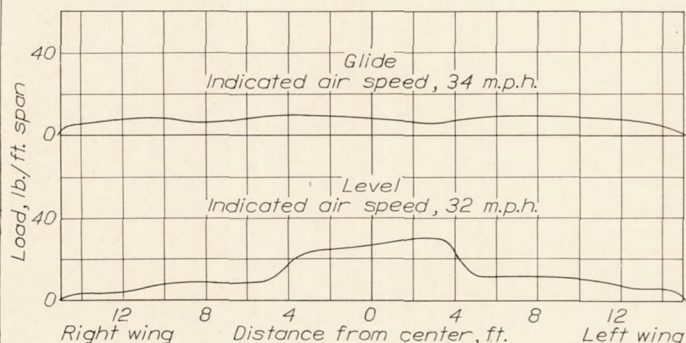
FIGURE 14.—Typical span-load curves—low speed (PCA-2 autogiro).

time. It can be stated that the coefficient a_0 represents the coning angle, or the average blade angle, and depends essentially upon the ratio between the thrust moment and the product of the blade moment of inertia and the square of the rotor angular velocity. The decrease in a_0 as the tip-speed ratio increases (figs. 5 and 8) indicates that the center of thrust of the individual blade approaches the axis of rotation. The coefficient a_1 represents the principal component of the flapping motion, and is caused entirely by the differences in resultant blade velocity at varying azimuth positions. The coefficients b_1, a_2, and b_2 represent the components of blade motion arising from the lag between the accelerating forces and the motion caused by them.

The effect of a constant acceleration on the force coefficients and blade motion is shown in figures 9 and 10, and the results indicate that the effect is a minor one. There is apparently a small consistent increase in the force coefficients, and a decrease in the coefficient a_1. The results were obtained in steady turns, however, and the additional angular velocity of the turn possibly influences the blade motion.

Accelerated flight.—At the beginning of the accelerated-flight tests it had been planned to obtain data on pull-outs and pull-ups. It was found, however, that an abrupt pull-out or pull-up resulted in the
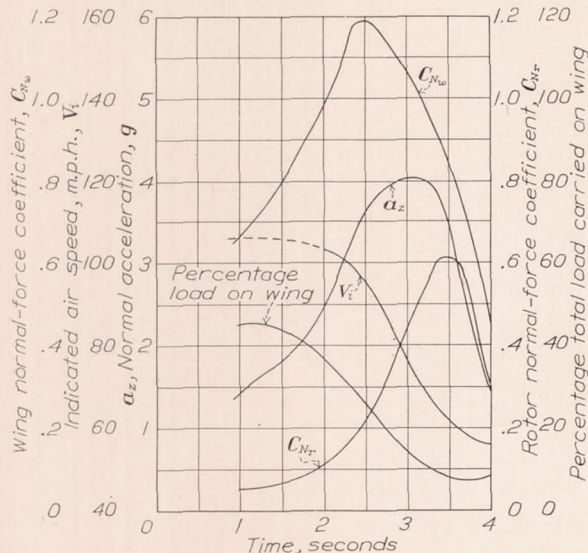

FIGURE 15.—Time history of abrupt turn, V_0=106 m.p.h. Weight=2,950 lb. (PCA-2 autogiro).
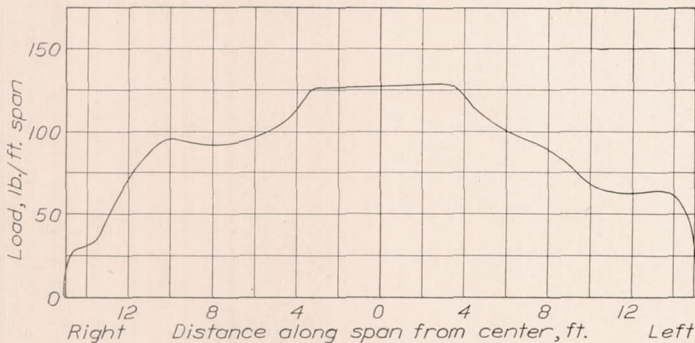

FIGURE 16.—Maximum span-load curve in abrupt turn, V_0=106 m.p.h. Time=2½ sec. (PCA-2 autogiro).

machine assuming an attitude that approached dangerously close to inverted flight, that is, inverted loading on the rotor. This condition is in no way similar to that passed through at the top of a loop, since the loading in a loop is at all times in a normal direction. The danger in inverted loading lies in the reversal of the coning angle, which endangers the tail surfaces. In order to avoid this situation, it was decided to perform abrupt vertically banked turns in a horizontal plane, since the data so obtained would be as valid a basis for design criterions as those obtained in maneuvers in a vertical plane.

Each of the four abrupt turns shown in the form of time histories (figs. 15, 17, 19, and 21) represents the most severe turn made in several trials at the same air speed. It will be noted that the maximum normal acceleration encountered was 4.3 g. Appreciable longitudinal instability was present at all times, even with the best obtainable center-of-gravity position, and may have imposed a limit upon the severity with which the test pilot performed the maneuver. During these tests, a change in instrument installation resulted in a rearward movement of the center of gravity of one half inch. The instability was immediately magni-

FIGURE 17.—Time history of abrupt turn, V_0=116 m.p.h. Weight=2,900 lb. (PCA-2 autogiro).
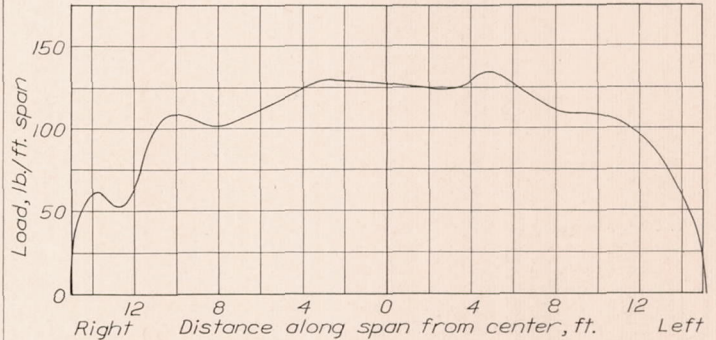
FIGURE 18.—Maximum span-load curve in abrupt turn, V_0=116 m.p.h. Time=2½ sec. (PCA-2 autogiro).

fied and manifested as a pronounced tendency for the machine to increase the severity of a turn against corrective control, combined with reversal of elevator stick force. This instability is considered a function of the individual design and not necessarily an inherent characteristic of the autogiro.

No consistent variation of maximum acceleration with air speed was observed during the tests, but the maximum wing load obtained was encountered in the highest speed turn. The results obtained indicate that it is possible for the wing to reach a normal-force coefficient of 1.0 or greater at a speed only slightly

FIGURE 19.—Time history of abrupt turn, V_0=126 m.p.h. Weight=2,910 lb. (PCA-2 autogiro).
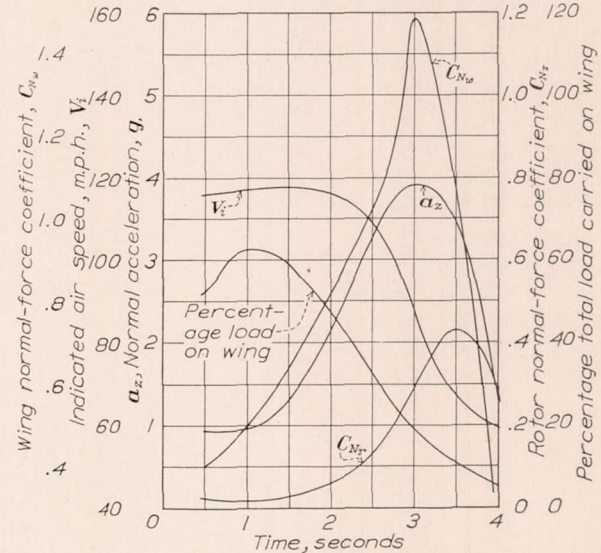

FIGURE 21.—Time history of abrupt turn, V_0=136 m.p.h. Weight=2,930 lb. (PCA-2 autogiro).

FIGURE 20.—Maximum span-load curve in abrupt turn, V_0=126 m.p.h. Time=2¼ sec. (PCA-2 autogiro).

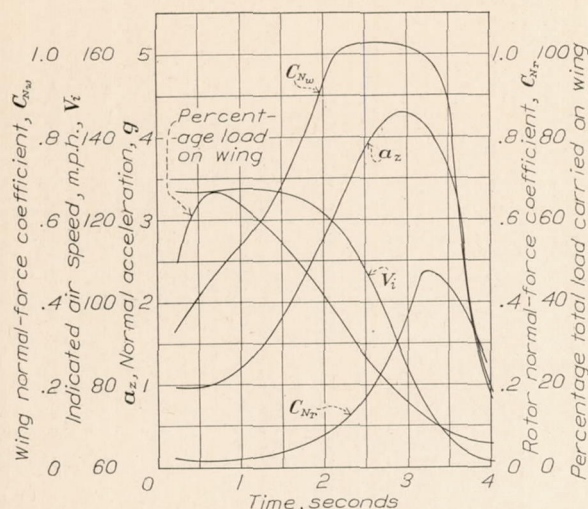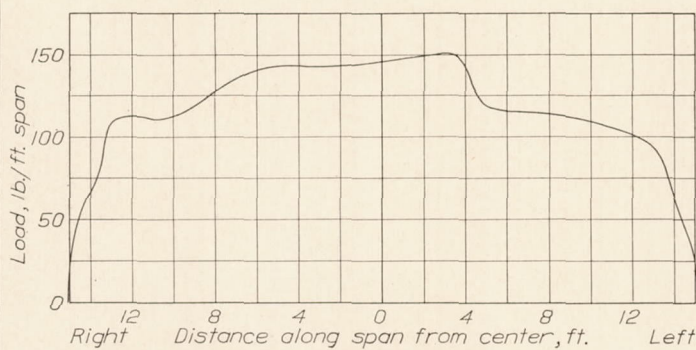
FIGURE 22.—Maximum span-load curve in abrupt turn, V_0=136 m.p.h. Time=3 sec. (PCA-2 autogiro).

lower than the speed at which the turn is started. The time histories presented show that in all cases when the acceleration had reached its maximum, the air speed had decreased materially and the rotor carried the major portion of the load. The maximum wing load was always reached before the maximum acceleration. The span-load curves shown in figures 16, 18, 20, and 22 indicate, if an allowance is made for the dynamic pressure increase in the slipstream, that the rib normal-force coefficient is approximately constant along the span. While no general conclusions may be derived from this, it indicates that the downflow from the rotor has an approximately constant effect over the entire wing.

CONCLUSIONS

1. The wing load varies in magnitude from 6 percent of the weight at low speed to 45 percent of the weight at high speed.

2. Variation of wing load with air speed is a major factor in determining the variation of rotor speed with air speed.

3. The effect of slipstream on the wing is sufficient to change the load carried by the wing by 7 percent of the weight.

4. The fixed wing will reach or exceed a normal-force coefficient of 1.0 in an abrupt turn at little less than the speed at which the turn is started.

LANGLEY MEMORIAL AERONAUTICAL LABORATORY,
    NATIONAL ADVISORY COMMITTEE FOR AERONAUTICS,
    LANGLEY FIELD, VA., *July 31, 1933.*

REFERENCES

1. Wheatley, John B.: Lift and Drag Characteristics and Gliding Performance of an Autogiro as Determined in Flight. T.R. No. 434, N.A.C.A., 1932.
2. Lock, C. N. H.: Further Development of Autogyro Theory. R. & M. No. 1127, British A.R.C., 1928.

TABLE I.—AUTOGIRO TEST RESULTS—STRAIGHT FLIGHT

Run no.	Maneuver	H Altitude (pressure) ft.	Δ Specific weight lb./cu. ft.	λ Attitude-deg.	θ Flight path angle deg.	α Angle of attack deg.	q Dynamic pressure lb./sq. ft.	N_r Rotor speed r.p.m.	μ Tip-speed ratio	W Weight-lb.	$C_{N'}$ Left wing panel	[1]C_{N_w} Wing normal-force coefficient	L Lift-lb.	L_w Wing lift-lb.	L_R Rotor lift-lb.	C_{L_r} Rotor lift coefficient	Coning and flapping angles				
																	a_0 deg.	a_1 deg.	b_1 deg.	a_2 deg.	b_2 deg.
1	Glide	4,000	0.0685	−14.1	−15.2	1.1	28.20	133.1	0.519	2,900	0.327	0.318	2,800	906	1,894	0.0423	5.07	5.03	3.95	0.70	−0.63
2	do	3,985	.0686		−23.8		42.2	117.0	.683	2,900	.298	.290	2,650	1,237	1,413	.0211	4.48	6.81	4.40	1.09	−1.22
3	do	4,070	.0671	−7.6	−12.1	4.5	12.38	142.2	.324	2,930	.429	.415	2,870	519	2,351	.1193	6.13	3.11	3.54	.26	−.11
4	do	4,120	.0676	−4.7	−10.7	6.0	7.12	143.6	.241	2,930	.581	.566	2,880	407	2,473	.218	6.42	2.30	3.29	.11	−.26
5	do	4,120	.0676	−3.2	−13.4	10.2	4.52	142.3	.192	2,900	.649	.639	2,820	292	2,528	.352	6.82	1.84	3.06	.17	−.17
6	do	3,950	.0674	−9.8	−13.5	3.7	18.77	141.5	.400	2,930	.376	.366	2,850	694	2,156	.0723	5.77	3.98	3.48	.32	−.40
7	do	3,975	.0674	−3.2	−13.7	10.5	4.63	142.3	.195	2,900	.723	.723	2,820	338	2,482	.337	7.03	1.53	3.19	.14	−.19
8	do	4,000	.0665	−5.9	−10.9	5.0	8.94	142.5	.275	2,930	.514	.499	2,880	450	2,430	.1710	6.49	2.43	3.49	.28	−.27
9	do	4,000	.0665	−2.7	−14.7	12.1	3.48	141.3	.170	2,900	.786	.786	2,810	276	2,534	.458	7.21	1.76	2.66	0	−.26
10	do	4,000	.0685	−1.8	−26.7	24.9	1.87	141.1	.114	2,930	.615	.600	2,610	113	2,497	.842	6.99	1.14	2.57	.02	−.09
11	do	4,000	.0685	−2.1	−23.7	21.6	2.34	140.4	.132	2,900	.559	.542	2,650	128	2,522	.678	6.97	1.05	2.66	.08	−.11
12	do	4,025	.0679	−2.1	−21.4	19.3	2.24	142.8	.129	2,930	.583	.568	2,730	128	2,602	.731	7.00	1.16	2.54	.06	−.16
13	Level	4,000	.0679		0		2.60	136.5	.147	2,900	1.264	1.118	2,900	277	2,623	.597	6.92	1.41	2.65	.06	−.04
14	do	3,990	.0702		0		3.43	134.4	.171	2,930	1.368	1.210	2,930	405	2,525	.435	7.04	1.24	3.23	.10	−.04
15	do	4,030	.0702	10.1	0	10.1	4.99	134.8	.209	2,900	1.158	1.023	2,900	504	2,396	.284	6.58	1.71	3.16	.22	−.02
16	do	3,970	.0694	7.4	0	7.4	7.43	131.8	.271	2,930	.852	.759	2,930	564	2,366	.1885	5.89	2.07	3.49	.20	−.10
17	do	4,000	.0694	3.2	0	3.2	19.00	131.7	.406	2,900	.502	.455	2,900	1,086	1,844	.0425	4.45	4.92	4.22	.89	−.38
18	do	4,000	.0682	2.5	0	2.5	25.7	125.6	.526	2,930	.459	.418	2,930	1,086	1,844	.0425	4.45	4.92	4.22	.89	−.38
19	Climb	4,050	.0680		4.5		8.84	129.0	.298	2,900	.852	.758	2,890	677	2,213	.1414	5.58	2.36	3.57	.27	−.03
20	Glide	4,050	.0688	−15.4	−16.2	.8	35.8	120.5	.645	2,930	.329	.320	2,810	1,157	1,653	.0300	3.88	5.44	4.58	1.06	−.43
21	do	4,100	.0688	−13.1	−13.4	.3	27.3	127.2	.533	2,900	.349	.340	2,820	963	1,857	.0428	4.35	4.56	4.00	.78	−.44
22	Climb	3,980	.0703	14.9	7.0	7.9	8.11	125.7	.287	2,930	.923	.820	2,910	672	2,238	.1632	6.25	2.13	3.48	.24	−.05
23	do	3,970	.0703		7.6		6.45	124.2	.259	2,900	1.153	1.020	2,880	665	2,215	.203	6.31	1.78	3.42	.24	.05

[1] Wing pressures were first determined completely only on the left wing panel. Subsequently, the total wing load was found as a function of the left panel load.

TABLE II.—AUTOGIRO TEST RESULTS—STEADY TURNS

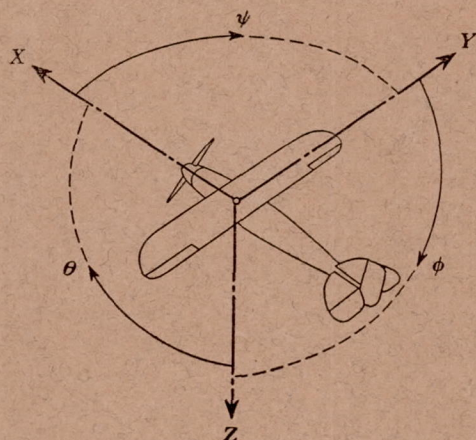| Run no. | Maneuver | H altitude (pressure) ft. | Δ Specific weight lb./cu. ft. | q Dynamic pressure lb./sq. ft. | N_r Rotor speed r.p.m. | μ Tip-speed ratio | a_z Normal acceleration g | a_x Longitudinal acceleration g | a_R Resultant acceleration g | α Angle of attack deg. | ϕ Angle of bank deg. | r Radius of turn ft. | W Weight lb. | N Normal force lb. | N_W Wing normal-force lb. | N_R Rotor normal-force lb. | C_{N_w} Wing normal-force coefficient | C_{N_r} Rotor normal-force coefficient | Coning and flapping angles |||||
|---|---|---|---|---|---|---|---|---|---|---|---|---|---|---|---|---|---|---|---|---|---|---|
| | | | | | | | | | | | | | | | | | | | a_0 deg. | a_1 deg. | b_1 deg. | a_2 deg. | b_2 deg. |
| 24 | Turn | 4,040 | 0.0700 | 13.47 | 157.2 | 0.302 | 1.45 | −0.09 | 1.45 | 6.4 | 46.5 | 369 | 2,930 | 4,250 | 1,009 | 3,241 | 0.742 | 0.152 | 7.50 | 2.31 | 3.69 | −0.01 | 0.16 |
| 25 | do | 3,840 | .0706 | 5.20 | 138.8 | .211 | 1.09 | −.23 | 1.11 | 10.7 | 25.8 | 306 | 2,900 | 3,160 | 512 | 2,648 | .975 | .321 | 6.58 | .15 | 3.56 | .06 | −.09 |
| 26 | do | 4,070 | .0671 | 7.54 | 146.3 | .244 | 1.27 | −.04 | 1.27 | 9.2 | 38.1 | 287 | 2,930 | 3,720 | 682 | 3,038 | .896 | .253 | 6.79 | 1.25 | 3.34 | .12 | −.05 |
| 27 | do | 3,840 | .0676 | 3.28 | 135.0 | .170 | 1.09 | −.18 | 1.10 | 15.0 | 24.8 | 211 | 2,900 | 3,160 | 460 | 2,700 | 1.387 | .518 | 6.80 | .60 | 3.22 | .15 | −.06 |

TABLE III.—ORIFICE PRESSURES

LEVEL FLIGHT—$q=34.2$ lb./sq. ft.
ABRUPT TURN—$q=39.2$ lb./sq. ft. (Initially 46.8 lb./sq. ft.)

Rib	Orifice no.	Pressure lb./sq. ft. level	Pressure lb./sq. ft. turn	Rib	Orifice no.	Pressure lb./sq. ft. level	Pressure lb./sq. ft. turn	Rib	Orifice no.	Pressure lb./sq. ft. level	Pressure lb./sq. ft. turn	Rib	Orifice no.	Pressure lb./sq. ft. level	Pressure lb./sq. ft. turn
A	1	39.0	101.3	E	1	58.3	155.0	H	1	75.0	145.0	K	1	70.0	175.0
	2	17.8	76.8		2	45.7	133.1		2	82.5	153.3		2	64.0	151.5
	3	6.3	29.2		3	39.0	98.0		3	52.4	86.0		3	38.4	90.0
	4				4	22.9	65.0		4	25.0	42.4		4	28.3	69.0
B	1	60.0	115.5		5	12.0	39.5		5	13.8	29.7		5	11.9	27.8
	2	35.0	88.0		6	−.4	10.6		6	7.4	24.5		6	−1.2	−.3
	3	11.0	32.5		7	−.7	2.8		7	2.2	18.0		7	−.3	.0
	4	6.4	14.9		8				8	−1.3	11.3	L	1	82.0	178.5
	5			F	1	56.2	159.0	I	1	60.0	137.5		2	67.5	152.5
C	1	65.0	189.2		2	53.3	146.2		2	55.0	138.7		3	46.5	108.0
	2	61.8	145.0		3	32.3	88.0		3	41.5	100.0		4	35.3	76.2
	3	51.0	137.0		4	21.4	62.4		4	20.0	58.0		5	15.5	22.7
	4	31.5	81.0		5	10.7	28.7		5	14.6	35.5		6	−1.0	.2
	5	11.3	31.3		6	7.2	14.4		6	5.7	10.5	M	1	60.7	123.8
	6				7	2.9	6.6		7	2.9	4.2		2	39.9	69.0
D	1	80.0	210.0		8				8	−.8	−1.7		3	15.9	33.0
	2	62.5	168.8	G	1	50.9	162.5	J	1	55.0	142.5		4	8.9	15.8
	3	44.8	120.5		2	55.1	166.0		2	61.0	128.7		5	.2	1.2
	4	31.5	47.0		3	30.1	105.0		3	37.0	101.5	N	1	48.0	69.0
	5	7.0	28.5		4	18.9	54.0		4	28.0	63.8		2	30.8	72.0
	6	1.5	4.2		5	6.2	.0		5	16.0	38.0		3	8.2	15.8
	7				6	6.4	15.3		6	5.7	17.0		4	2.8	4.5
					7	1.0	5.4		7	.9	2.6				
					8	3.0	4.5		8	−.8	−1.4				

Positive directions of axes and angles (forces and moments) are shown by arrows

Axis		Force (parallel to axis) symbol	Moment about axis			Angle		Velocities	
Designation	Symbol		Designation	Symbol	Positive direction	Designation	Symbol	Linear (component along axis)	Angular
Longitudinal___	X	X	rolling_____	L	$Y \longrightarrow Z$	roll_____	ϕ	u	p
Lateral_____	Y	Y	pitching____	M	$Z \longrightarrow X$	pitch_____	θ	v	q
Normal_____	Z	Z	yawing_____	N	$X \longrightarrow Y$	yaw_____	ψ	w	r

Absolute coefficients of moment

$$C_l = \frac{L}{qbS} \qquad C_m = \frac{M}{qcS} \qquad C_n = \frac{N}{qbS}$$

Angle of set of control surface (relative to neutral position), δ.   (Indicate surface by proper subscript.)

4. PROPELLER SYMBOLS

D,   Diameter.

p,   Geometric pitch.

p/D, Pitch ratio.

V',   Inflow velocity.

V_s,   Slipstream velocity.

T,   Thrust, absolute coefficient $C_T = \dfrac{T}{\rho n^2 D^4}$

Q,   Torque, absolute coefficient $C_Q = \dfrac{Q}{\rho n^2 D^5}$

P,   Power, absolute coefficient $C_P = \dfrac{P}{\rho n^3 D^5}$.

C_S, Speed power coefficient $= \sqrt[5]{\dfrac{\rho V^5}{P n^2}}$.

η,   Efficiency.

n,   Revolutions per second, r. p. s.

Φ,   Effective helix angle $= \tan^{-1}\left(\dfrac{V}{2\pi r n}\right)$

5. NUMERICAL RELATIONS

1 hp = 76.04 kg/m/s = 550 lb./ft./sec.

1 kg/m/s = 0.01315 hp

1 mi./hr. = 0.44704 m/s

1 m/s = 2.23693 mi./hr.

1 lb. = 0.4535924277 kg.

1 kg = 2.2046224 lb.

1 mi. = 1609.35 m = 5280 ft.

1 m = 3.2808333 ft.